Metrol. Meas. Syst., Vol. 32 (2025) No. 4, pp. 1–17
DOI: 10.24425/mms.2025.155800

PAN POLSKA AKADEMIA NAUK

METROLOGY AND MEASUREMENT SYSTEMS
Index 330930, ISSN 0860-8229
www.metrology.wat.edu.pl

M&MS

RECEIVER NETWORK FOR ASSESSING THE ACCURACY OF TIME DISTRIBUTION IN E-CZAS RADIO SERVICE

Jarosław Sadowski

Gdansk University of Technology, Department of Radiocommunication Systems and Networks, ul. Narutowicza 11/12, 80-233 Gdansk, Poland (✉ *jarsadow1@pg.edu.pl*)

Abstract

E-Czas Radio is a service for distributing official Polish time data using a long-wave AM broadcast transmitter operating at 225 kHz. Although the system is still being developed, it already offers the possibility of distributing time with accuracy exceeding the operator's initial declarations. However, an independent assessment of the quality of time dissemination and the possible accuracy of end-user device synchronisation will be required to verify the system assumptions and estimate the system performance characteristics. Therefore, a set of measuring receivers for detecting time messages and measuring the message time of arrival has been built at the Gdansk University of Technology. This paper presents the proposed method for signal processing and message time detection, along with the results of preliminary tests on the quality of time and frequency sources used as references for the evaluation of e-Czas time data and the relative errors of message detection times between different receivers.

Keywords: Radiocommunication, synchronisation, time distribution.

1. Introduction

Accurate and reliable time information is essential for the correct operation of many technical systems. Telecommunication networks, power grids, banking processing systems, etc. must be synchronised, and the required reliability of time synchronisation is increasing as these systems become more important and more complex. Accurate device synchronisation and time measurements are essential parts of time-based positioning systems, which is why, in addition to the basic positioning and navigation services, a time distribution service is offered, for example, by all time-based *global navigation satellite systems* (GNSS), such as *Global Positioning System* (GPS), Galileo, and Beidou. In fact, GNSS-based time distribution is often considered the easiest to use due to almost global GNSS coverage and the high availability of relatively inexpensive GNSS-disciplined clocks, both in the form of standalone devices and modules for integration with other equipment. However, the most important advantage of GNSS-based time synchronisation is its accuracy, which can reach the nanosecond level, high enough for most applications. Unfortunately, reception of GNSS signals is limited mainly to outdoor environments due to the low signal power at ground level

Article history: received April 15, 2025; revised June 12, 2025; accepted July 25, 2025; available online September 19, 2025.

and the high attenuation of GNSS frequencies by buildings and construction materials. Receiving GNSS signals indoors using mobile devices usually requires some additional fixed infrastructure, *i.e.* signal repeaters, which makes such a solution more difficult to implement. In addition, GNSS signals can be easily jammed, which can lead to the inaccessibility of both position and time data [1, 2]. This deliberate jamming and spoofing has recently been observed in large parts of Eastern Europe and the Middle East [3]. Some GNSS signal jamming incidents have also been reported in South Korea. Therefore, in some applications, other independent sources of time data may be required. Considering the high attenuation of *radio frequency* (RF) signals in the *ultra-high frequency* (UHF) band in buildings and susceptibility to interference caused by low signal power levels, time distribution systems that utilise the *low frequency* (LF) band can be an interesting alternative to GNSS-based time synchronisation. Time synchronisation can also be achieved using network-based solutions and the *Network Time Protocol* (NTP) [4] or *Precision Time Protocol* (PTP) [5] protocols. The NTP protocol allows one to achieve millisecond-level accuracy using global networks [6], even mobile networks such as 4G/*Long Term Evolution* (LTE) [7], and tens of microseconds in the case of local networks, but its performance depends on the communication network parameters such as bandwidth or variable latency [8]. In applications that require a high level of reliability, dedicated solutions for time dissemination are implemented. An example of device synchronisation via the power grid can be found in the publication [9], together with a comparison of requirements regarding the accuracy of synchronisation for different purposes. A much higher accuracy of time synchronisation between network-enabled devices should be provided by PTP-based equipment [10], but the quality of sub-microsecond synchronisation in PTP requires dedicated network equipment (switches, routers) and stable communication link parameters. Both network-based synchronisation methods require a bidirectional communication channel in the form of some kind of computer network, but in applications where such communication is not available radio-based time dissemination services that use low-frequency band may still be the best option.

The LF band is defined by the International Telecommunication Union as the frequency range between 30 kHz and 300 kHz [11]. For example, DCF77 operates in this band, which is the most widely known time data transmitter in Europe, located near Frankfurt in Germany. The DCF77 uses the 77.5 kHz carrier with combined *amplitude shift keying* (ASK) modulation used to encode date, time, and additional information by changing the duration of carrier emission with reduced power, and with additional *phase shift keying* (PSK) modulation for more accurate detection of signal time of arrival and higher accuracy of time synchronisation [12]. This additional PSK modulation allows us to achieve a standard deviation of time synchronisation that is better than 20 microseconds [13]. A similar data frame structure, but a different modulation scheme (PSK), is used by another European time transmitter ALS162 in Allouis, France [14]. The ALS162 is declared to provide time accuracy of no worse than 1 ms [15]. Both consumer-grade and industrial-grade receivers for time synchronization using DCF77 and ALS162 are commercially available [16, 17]. The International Bureau of Weights and Measures provides annual reports [18] with a brief description of other active time signal transmitters and authorities responsible for their operation and maintenance. However, most of them are located outside Europe.

In addition to dedicated time dissemination transmitters, such as DCF77 and ALS162, time data can also be found in the LF band in the signal of some Loran-C transmitters. Although almost all American and European Loran transmitters ceased operation in 2010 and 2015, respectively, there are still a few transmitters active, including the transmitter at Anthorn, UK. This transmitter operates in e-Loran mode with additional pulse position modulation for data transmission and transmits time data, as well as differential corrections for GNSS-based time dissemination and positioning. E-Loran receivers for time synchronisation are also commercially available [19, 20], therefore, Loran-based time dissemination is ready for use, although in practice it is not very common.

The signal from the German DCF77 transmitter can be received in Poland, but the increasing level of industrial interference in the LF band, observed in urban environments, together with the high variability of the LF radio signal propagation characteristics makes it difficult to use the DCF77 signal during the day. Stable reception of the ALS162 or Loran signal from Anthorn in Poland is even less possible. But at the end of 2023, the Polish *Central Office of Measures* (COM) announced the start of the transmission of Polish time data in the "e-Czas Radio" ("e-Time Radio") service using the AM broadcasting transmitter in Solec Kujawski (Poland) at 225 kHz frequency [21]. This transmitter is a broadcast transmitter that uses the standard *double-sideband amplitude modulation* (DSB AM) to transmit the audio signal of the Polish Radio Programme One. High transmitter power, up to 1.2 MW and a dual-antenna array (330 m and 289 m) for the directional radiation pattern, which compensates for the non-central position of the transmitter facility in Poland, guarantee stable signal reception throughout the country both during the day and at night [22]. Polish official time data are transmitted using additional phase shift keying modulation, the parameters of which have been selected to reduce the risk of mutual interference between AM modulation sidebands with the audio signal and PSK-modulated data packets. Although the time dissemination service is called e-Czas Radio, the emission of time data is presented in the technical literature as "PCSK225" [23]. The signal structure and modulation parameters are briefly presented in Section 2. The Central Office of Measures declares the possibility of achieving an end-user device synchronisation accuracy of no worse than 10 ms [23]. Although initial tests performed in 2024 have shown that radio packets with time data are transmitted irregularly, the LF transmitter has recently undergone a significant update and now allows for stable reception of time data with millisecond accuracy. Therefore, the "e-Czas Radio" system is ready to be used, but no reliable data on its performance in time dissemination are yet available.

Although the e-Czas service is relatively new, the first devices that use data transmitted from Solec Kujawski for time synchronisation are already developed and available on the market [24]. However, before this new source of Polish official time can be used by the government, administration, industry, or academia, the actual quality of time dissemination and the possible accuracy of end user devices synchronisation must be assessed. For this purpose, a set of time data receivers was designed and built at the Gdansk University of Technology, which allows measuring the time of arrival of phase-modulated time data packets and estimating the absolute and relative accuracy of time dissemination. The development and construction of the receiver network was carried out within statutory activities of the Gdansk University of Technology, and the author is in no way associated with the Central Office of Measures. Therefore, the developed devices can be used for an independent, objective assessment of the quality of time data transmission using a long-wave transmitter at 225 kHz.

The block diagram of the proposed receiver network for the evaluation of the e-Czas Radio time dissemination service is shown in Fig. 1. Currently, a set of four receivers has been built as the minimum number of devices that enables simultaneous, synchronous reception of the 225 kHz signal from Solec Kujawski in four locations:

- a stationary receiver in close proximity to the transmitter – reference measurements to assess the effects of mixed AM DSB and phase modulation.
- two stationary receivers in urban and rural areas at a similar distance from the transmitter – to evaluate the effects of man-made interferences.
- a receiver installed in different locations to evaluate the quality of time synchronisation depending on distance and terrain type.

The receivers are connected to the central database via an IP link, using *e.g.* a cellular network or a fixed network. However, the design and implementation of the central database and communication is straightforward, and the description of this part of the receiver network would

not bring any new knowledge to the field of measurement techniques. Therefore, this article mainly focuses on the description of the e-Czas Radio signal structure, the design of measuring receivers, and the signal processing methods implemented in these receivers to measure the time of arrival of the e-Czas Radio messages.

The rest of the article is organised as follows: The structure of the e-Czas Radio signal is briefly presented in Section 2, with a discussion of the unclear and yet undefined details of the signal structure or reception method. The next section describes the receivers developed for the evaluation of characteristics of the time dissemination service. A discussion of the possible accuracy of estimation of the e-Czas signal parameters is presented in Section 4. The last section concludes the paper.

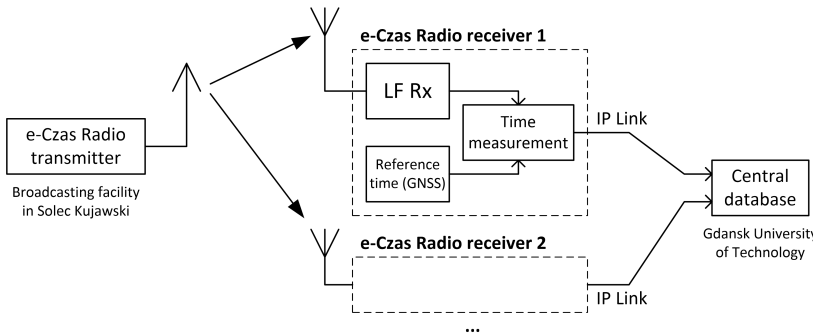

Fig. 1. Block diagram of the receiver network for e-Czas Radio time dissemination performance assessment.

2. Time signal structure

The description of the e-Czas Radio signal structure is based on the signal specification [25] published on the project website and the official English translation of the specification [26] together with the documentation of an exemplary receiver [27], which are available on GitHub.

A one-minute frame is divided into 20 time slots, counted from 0 to 19, each slot lasting 3 seconds. The time slot number 0 starts at the beginning of a new minute. Messages are sent at a bit rate of 50 bps and consist of 96 bits, so their duration is 1.92 s, which is shorter than the duration of one slot. The signal specification does not indicate the timeslot to be used for time data transmission, but since the time message contains a timestamp field with 3-second resolution, equal to the duration of the time slot, time data messages can be transmitted in any time slot within a frame. In the current system implementation, packets with official time are transmitted irregularly and number of slots in a frame with time data varies from 1 to over 10, but it is confirmed from observations that at least one time packet is transmitted in each minute. Other slots can be used for transmission of other messages, not related to time dissemination, but only the format of the time data message is covered by the specification [25] and [26].

Messages sent in the e-Czas Radio system consist of 96 bits, of which only 37 contain official Polish time and supplementary data. The structure of the official time messages is shown in Table 1 [26]. The third field with the fixed sequence “101” is used as a reference point for the timestamp data encoded in the 30-bit field S0 to S29: the start of the symbol “0” in this sequence is delayed by exactly 0.5 second from the nominal transmission time of the packet, indicated by the timestamp. Considering that “0” in the “101” sequence is preceded by 25 symbols, each with a duration of 20 ms, which means that, as expected, the timestamp data refer to the start of the entire message transmission.

Although almost the entire message is coded using the *Reed-Solomon* (R-S) error correction code, the specification [26] does not disclose any parameters of the R-S code. It is somehow surprising that the R-S code includes only 36 bits from bit S0 to SK0, but not the SK1 bit. Furthermore, also the 8-bit *cyclic redundancy code* (CRC) checksum parameters (polynomial) are not presented in [26]. Some information on the R-S code parameters can be found in the reference receiver documentation [27]. It has been experimentally shown that actual messages received from Solec Kujawski are encoded using a polynomial "19" which is equal to $D^4 + D + 1$, and the initial root is equal to 9. All recorded time data packets had the CRC field that matches the polynomial $x^8 + x^2 + x + 1$, known as CRC-8 CCITT, with the initial state of the shift register equal to all "0".

Table 1. Structure of messages with time data.

Field length [bits]	**Field name(s)**	**Description**
16	–	Preamble: fixed synchronisation pattern (0x5555, MSB first)
8	–	Fixed start of frame delimiter, message ID (0x60, MSB first)
3	–	Fixed sequence "101" which indicates a reference point for time synchronisation
30	S0 to S29	Timestamp expressed in three-second periods counted from Jan. 1, 2000
2	TZ0, TZ1	Local time shift, 00 = no shift, 10 = +1 hour, 01 = +2 hours, 11 = +3 hours
1	LS	Bit indicating announcement of introduction of a leap second
1	LSS	Bit indicating leap second sign
1	TZC	Bit indicating upcoming summer/winter time change
2	SK0, SK1	State of LF transmitter in Solec Kujawski, 00 = normal operation, 10 = planned shutdown for one day, 01 = planned shutdown for a week, 11 = planned shutdown for more than a week
24	RS ECC	Reed-Solomon error correction bits
8	CRC-8	Checksum

According to the specification, time messages are scrambled before transmission by calculating the modulo-2 sum with the fixed sequence 0x0a47554d2b, but the purpose of this scrambling is not defined. It has been observed that even with this scrambling, long streams of "zeros" and "ones" are possible in scrambled messages, therefore, this scrambling does not guarantee a large (or constant) number of phase transitions in radio packets, which could potentially improve the quality of time of arrival measurements.

A sample time message from Solec Kujawski, recorded using one of the receivers presented in the next section, is shown in Fig. 2. This graph presents the instantaneous carrier phase as a function of time with respect to the unmodulated carrier phase observed before message transmission began. It may be a little surprising that carrier phase modulation is unipolar with negative phase shift only, as such phase bias may theoretically alter functioning of some synchronous receivers with carrier recovery, but the vast majority of AM broadcast receivers use envelope AM detectors that are not susceptible to carrier phase modulation. Thus, such phase modulation has no effect on the main emission of double-sided AM modulation and reception of the public radio broadcast service.

The published e-Czas Radio signal specification [26] lacks some important information, crucial for the correct design and implementation of the time distribution receiver. The first missing data are the carrier phase modulation parameters. Some details about carrier modulation are only included in the exemplary receiver documentation [27]: the carrier phase shift is negative:

$-36° \pm 3.6°$ with a linear phase transition between opposite symbols and the plot in Fig. 2 confirms these parameters, but the phase change ratio is not defined. Instead, there is a disclaimer that the modulation parameters may be changed in the future. During correspondence, the Central Office of Measures stated that the time of linear phase transition between symbols is currently set to 19 ms, but the author was informed that the modulation parameters are not fixed and can be changed in future to tune the system for best performance.

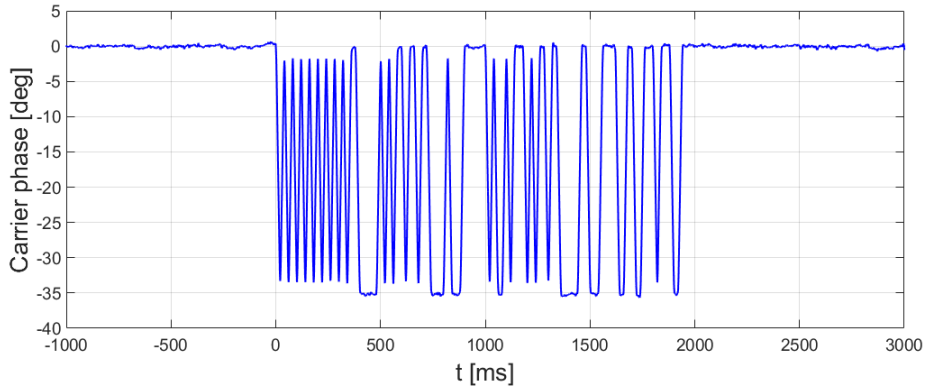

Fig. 2. Carrier phase modulation of the LF transmitter at 225 kHz – time data.

Other important missing information is the description of the reference method of measuring the signal time of arrival, which should be used in order to get the highest accuracy of time synchronisation. Implementation of another detection method, which was not considered by the system designer, especially since the exact shape of the transmitted messages has not yet been precisely defined, can cause both systematic and random errors and significantly affect the results of the evaluation of performance of the e-Czas Radio system. Therefore, the structure of the measuring receivers, described in Section 3, was designed taking into account the experience gained in the construction of receivers for time-based positioning systems, with particular emphasis on the possibility of easy updating of the method of detection of the signal time of arrival, which is performed in the software.

3. Measurement receivers for evaluation of time signal parameters

Although the e-Czas Radio service is advertised as a solution which allows us to get time synchronisation no worse than 10 ms, one can expect a much better accuracy, at least by an order of magnitude, especially in good propagation conditions. Therefore, the receivers for evaluating the system parameters must be able to demodulate the carrier phase from the LF signal at 225 kHz in the presence of AM modulation sidebands, detect the beginning of the data messages, and measure the time of arrival of the signal with respect to an external, high-quality time reference, with a resolution and accuracy much better than 1 ms. Taking into account the arguments presented in Section 1, a GNSS-disciplined oscillator, capable of providing both a highly stable 10 MHz clock for driving the receiver and 1 *pulse per second* (PPS) pulses for precise time synchronization, was selected as the source of the time and frequency reference.

The relatively low frequency of the signal from the transmitter in Solec Kujawski allows the use of a direct sampling receiver structure without the need for any analogue frequency conversion. The direct sampling receiver has some advantages that can be important in implementation of

the receiver for assessing the quality of time data, such as very limited distortion of the signal phase characteristics due to analogue filtering limited only to a wideband anti-aliasing filter before an *analogue to digital converter* (ADC), with almost linear phase characteristics in the passband. All other signal processing is done in the digital domain, which ensures stable and predictable delays, and in the case of *finite impulse response* (FIR) digital filters: also, perfectly linear phase characteristics. Therefore, direct sampling LF receivers were needed, which allows synchronisation of signal sampling with external time reference. Despite the large selection of *software-defined radio* (SDR) devices, only few of them cover the low-frequency band. For example, the Ettus Research USRP N200 [28] equipped with an LFRX daughterboard [29] works in the frequency range from 0 to 30 MHz, but the LFRX board contains only buffers with unity gain, connected directly to the inputs of the ADC converter. Therefore, this SDR platform offers very poor sensitivity, about –45 dBm, and because it only performs ADC operation, all additional data processing (frequency conversion, filtering, phase estimation) must be performed on a PC computer. In fact, the N200 with LFRX daughterboard was used to create the first prototype of the software-based e-Czas radio signal receiver, but the need for external filters and preamplifiers, as well as the high requirements for the computing power of the PC, made this solution unfavourable, and that is why the USRP-based e-Czas receiver is not presented here. Another SDR receiver, called KiwiSDR [30], has all the required RF filters and preamplifiers already built in, but since it was designed to work as a remotely-controlled receiver for radio amateurs, implementing e-Czas PL reception using this device would require the preparation of new firmware and FPGA code. It is also uncertain how good time synchronisation would be achieved using the built-in GPS receiver. However, considering the advantages and disadvantages of the various SDR devices available on the market, the e-Czas Radio signal receivers were designed similarly to the KiwiSDR receivers. The main component of the receivers is a Zynq chip, which consists of an FPGA and an ARM processor, allowing the use of fast and highly predictable digital signal processing in the FPGA together with the flexibility of software-based signal processing in the ARM processor running Petalinux. The block diagram of the receivers is presented in Fig. 3.

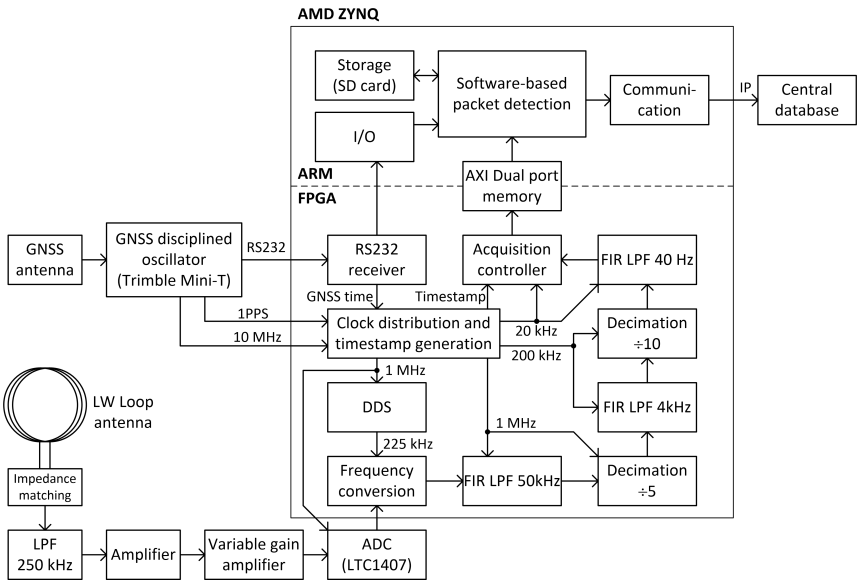

Fig. 3. Block diagram of the e-Czas Radio signal receivers.

The loop antennas were chosen to receive 225 kHz LF signals. The antennas consist of 3 turns of wire on a 30 cm diameter inside a copper shielding tube, and they are not tuned to resonance to provide the flattest possible phase response near the frequency of the signal with time data. The signals from the antennas are filtered using 5th order LC low-pass filters with a cut-off frequency of 250 kHz. The signals are then amplified in a two-stage wideband amplifier with fixed gain and in a *variable gain amplifier* (VGA). All of these amplifiers are used to provide a signal level suitable for the analogue-to-digital converter, but since phase demodulation is not vulnerable to signal amplitude change over a wide range, automatic gain control is not needed. Thus, the VGA is used only to manually set the overall path gain during receiver installation to ensure correct operation, and the VGA gain is then kept constant during receiver operation.

After amplification, the signals are sampled and converted to the digital domain using an LTC1470 ADC, clocked at a sampling rate of 1 MHz. Next, the real-valued digital signal is downconverted from 225 kHz to a complex baseband signal using a 225 kHz complex harmonic signal generated by a *digital direct synthesis* (DDS) block implemented in the FPGA. The signal carrier frequency and the sampling frequency have a rational ratio of 9/40, therefore, generating the local oscillator signal using DDS does not introduce any frequency rounding errors. The next step in digital signal processing, before phase detection, is to remove the AM sidebands, which should occupy the spectrum between 100 Hz and 4.5 kHz. This can be done using low-pass filters with a cut-off frequency of 40 Hz, as shown in the simplified block diagram in Fig. 4a. The cut-off frequency was manually selected as the lowest value that does not reduce the carrier phase peak-to-peak deviation value during the reception of the packet preamble, selected for time of arrival measurements. However, with such a low cut-off frequency, high requirements on the filter transition band, and a relatively high sampling rate of 1 MHz, the required finite impulse response filter length is about 20000. Such a long impulse response causes high demands on computational resources and the output signal, with bandwidth limited to 40 Hz, is unnecessarily oversampled. Therefore, digital signal filtering is divided into three stages, as shown in the block diagram in Fig. 4b. The first filter is a low-pass FIR filter with a cut-off frequency of 50 kHz, which processes signal samples with a sampling rate of 1 MHz. Then the signal is decimated by a factor of 5 to obtain a lower sampling rate equal to 200 kHz. The second FIR filter has the cut-off frequency of about 4 kHz, and the signal from the output of this filter is decimated again, this time by a factor of 10. Finally, the signal with a sampling rate of 20 kHz is filtered by a third FIR filter with the final cut-off frequency of 40 Hz. Although this signal processing chain may seem complicated,

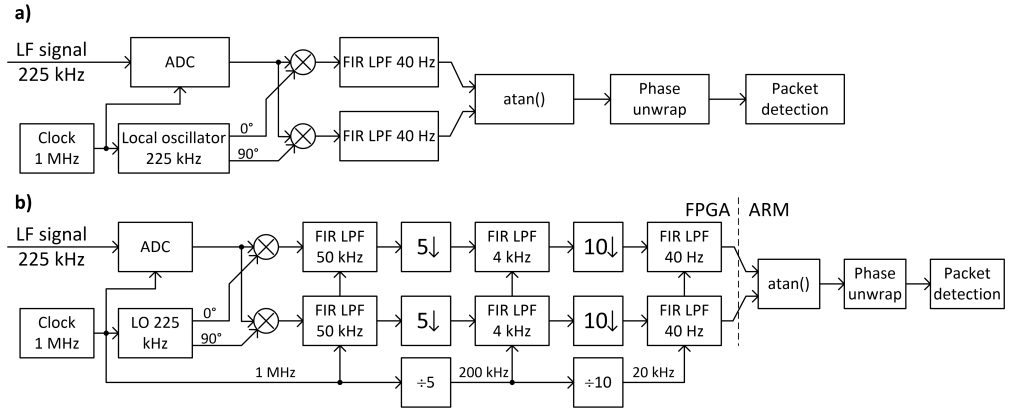

Fig. 4. General concept (a) and real implementation (b) of digital signal processing in the LF receiver.

it allows for a significant reduction in the total number of signal multiplications, firstly because the sum of the impulse response lengths of all three implemented FIR filters (101+501+3001) is lower than the required filter length in the case of single-step filtration and secondly because many operations are now performed using the lower sampling rates of 200 kHz and 20 kHz.

The phase detection of the low-pass filtered baseband equivalent of the 225 kHz carrier signal is performed using a four-quadrant arctangent function, and time data packets can be detected after phase unwrapping. However, unlike signal downconversion, decimation, and filtering, which should remain unchanged even if the e-Czas Radio system operator introduces some changes to the signal modulation parameters, the method of packet detection and time measurement can be highly dependent on modulation details that have not yet been defined in the published system specification. Therefore, all signal processing steps after the final low-pass filtering are performed in software, which is why the receiver block diagram shows a buffer between the FPGA part and the ARM processor just after the last FIR low-pass filter. The stream of complex baseband signal samples from the FPGA is divided into blocks of 1000 samples (50 ms) and mapped to the ARM virtual memory space for further software-based processing.

All signal processing blocks in the FPGA are driven by clocks derived from an external 10 MHz clock from a Trimble "Mini-T GG" GNSS disciplined oscillator. This GNSS receiver also provides a 1 PPS signal, which, together with the GPS date and time, decoded from messages sent over the RS232 interface, allows one to attach a timestamp to all signal samples with a resolution of 50 μs. The sample timestamp resolution is defined by the sampling rate of the last decimation stage in the FPGA, but the accuracy of the signal sampling and the timestamp is defined by the quality of the GNSS receiver. Trimble declares that the standard deviation of error of the 1 PPS pulses with respect to the GPS system time is about 15 ns (1σ), which is over three orders of magnitude better than the final sampling period and about five orders of magnitude better than the expected accuracy of time dissemination in the e-Czas system.

The specification [26] does not describe any reference method for estimating the signal time of arrival. However, given the general description of the message format and the observed phase plots from currently transmitted messages, a simple method has been proposed to measure the message time, which is based on the synchronisation sequence from the packet preamble. The preamble consists of 16 bits that form a sequence of alternating bits "0" and "1" (Table 1). Figure 2 shows that this sequence forms a highly repeatable waveform with an almost triangle-like shape. Given the available details of the signal structure, the ideal carrier phase diagram should look as shown in Fig. 5a: the change from bit "0" to "1" and vice versa consists of a linear phase change that takes 19 ms, followed by a stable phase value during the last 1 ms in a 20 ms long symbol. The system specification does not define whether the symbol start time is counted from the beginning of the linear phase change, as presented in Fig. 5a, or from the time when the phase value crosses a threshold of half the value between the carrier phase corresponding to "0" and "1" (–19° relative to the unmodulated carrier phase). When designing the receiver software, the author assumed that the phase change starts at the beginning of the symbol duration time, but if the latter possibility is true, there will be a constant time error of 9.5 ms, which will be easy to detect and compensate for.

Multiple signal filtering steps on the transmitter side as well as in analogue and digital filters on the receivers remove all sharp transition between different parts of symbols and create distinct maxima and minima in the instantaneous carrier phase plots as shown in Fig. 5b. By using FIR digital filters with a symmetric impulse response shape, local maxima and minima should occur exactly in the middle of a symbol time period with a theoretically constant carrier phase, which should be 19.5 ms after the start of the nominal symbol duration time. Therefore, a simple algorithm for estimating the message time of arrival is proposed, which is based on detecting the occurrence of local phase maxima/minima (carrier phase value peak detection) near the end

of bits number 2 to 15 in the message preamble sequence. When t_n is the detection time of the maximum/minimum phase at the end of bit n for $n = 2 \ldots 15$, the message start time T is calculated by averaging the detection results compensated by the duration of the previous symbols:

$$T = 0.5 + \frac{1}{14} \sum_{n=2}^{15} (t_n - 20 \cdot n) \ \ [\text{ms}]. \tag{1}$$

It has been tested in practice that even without external interferences, noise generated by preamplifiers and quantisation noise in ADC is sufficient to create conditions for quantisation dither, which allows for sub-sample time measurement resolution. The message time detection method can also be based on cross-correlation of the received preamble and a locally generated signal template with a fractional delay for sub-sample resolution; however, it has been checked that correlation-based detection is more demanding in terms of computational resources but does not allow for a statistically significant improvement in the accuracy of time estimation compared to peak detection. In contrast, the threshold crossing method may be less accurate due to its possible vulnerability to the nominal phase deviation value that may be changed in the future, and for this reason, it is not recommended.

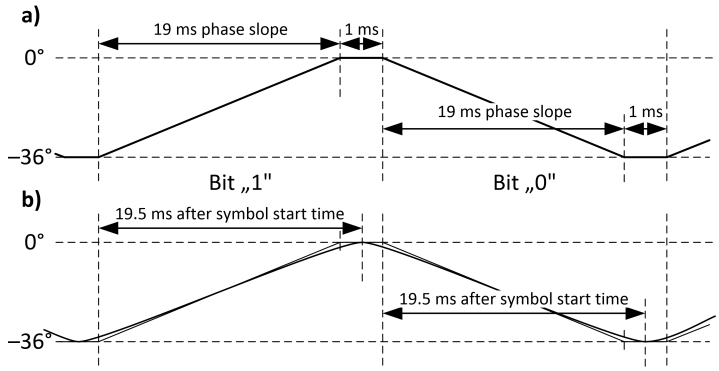

Fig. 5. Theoretical shape of the carrier phase a) and the model used for detection of the message time b).

After successfully detecting the message and measuring the time of arrival, the received packet is demodulated and decoded according to the encoding rules described in Section 2. When the CRC-8 checksum value is correct, the decoded message and the results of the measurement of signal time of arrival are sent to the central database. Optionally, samples of the recorded signals can also be sent for further evaluation of the quality of the time data signal.

By splitting the digital signal processing between a hardware implementation in the FPGA part of the Zynq XC7Z020 "System on Chip" (Artix-7 structure, 85k logic cells) and a software implementation using the dual-core ARM processor in the Zynq chip, a high degree of flexibility is achieved in the design and implementation of message time of arrival detection. The message detection, decoding, parameter measurement, and communication with the central database use only a little over 7% of the processor's computational capability, including the overhead caused by the Linux system. All receivers were built using commercially available "Zedboard" development boards connected to custom boards with analogue filters, preamplifiers, ADC converters and input/output interfaces for communication and clocking the Zynq with GNSS clock. Currently, a set of four receivers is completed together with a simple database on a central server for storing and processing data. All receivers communicate with the server using an IP link. The development

boards are equipped with a 1 Gb Ethernet interface that can be connected to almost any type of IP network available at the measurement site. The prototypes are also equipped with a 3G/4G cellular router. Transmission of measurement results generates less than 1 MB of traffic per day; the additional transmission of signal samples increases the traffic to about 250 MB per day.

4. Tests

Before the receivers were installed in the planned signal recording locations, it was necessary to test their correct operation, especially in terms of signal detection time measurements.

4.1. Verification of performance of GNSS disciplined clocks

The e-Czas signal receivers use Trimble "Mini-T GG" GNSS disciplined oscillators as the main sources of both reference frequency, used for RF signal frequency conversion and ADC clocking, and reference time, used for sampling synchronisation and estimation of the detection time of e-Czas radio packets. Therefore, the parameters of these GNSS clocks directly influence the receiver performance. Trimble declares short-time standard deviation of the 1 PPS pulses at the output of GNSS clock to be no worse than 15 ns ($1\,\sigma$) [32]. However, since the devices used to build the receivers are not new (in fact, they are no longer offered by Trimble), they had been tested for correct operation by comparing the 1 PPS outputs from two GNSS clocks with 1 PPS pulses generated by an FS725 free-running rubidium clock [31], which is one of possible procedures for GNSS clock verification described in [33] and was also used for GPS-based timing evaluation in [34]. The two tested GNSS receivers used different antenna placements: on the roof top with a clear view of the sky and on a windowsill with only half of the sky visible. The results obtained from several days of observation are summarised in Table 2.

Table 2. Verification results for the performance of GNSS-disciplined clocks.

GNSS clock antenna placement	Standard deviation of 1 PPS error	Maximal error of 1 PPS signal
Roof top (clear sky view)	14.5 ns	44 ns
Windowsill (half sky view)	20.8 ns	177 ns

The reference time accuracy of both tested GNSS disciplined clocks is fully comparable with typical values for GPSDO presented in Appendix B of the publication [33] and is more than five orders of magnitude better than the declared accuracy of the e-Czas Radio service. However, GNSS-based receiver synchronisation may be further improved, *e.g.*, by using high accuracy GNSS services [35] or an additional 5G link for clock offset data exchange [36]. Therefore, synchronisation of receiver operation using GNSS clocks does not compromise their ability to precisely measure the e-Czas signal time of arrival, and even the installation of a GNSS antenna without a clear sky view allows to achieve sufficient reference clock accuracy.

4.2. Evaluation of performance of the time data receiver

The e-Czas Radio service is relatively new and is not yet widely known; therefore, none of test equipment available on market directly supports testing time dissemination receivers. However, the repetitive structure of the e-Czas messages allows for easy generation of the test signal using an R&S SMU200 vector signal generator with a built-in baseband arbitrary waveform generator. For

the tests, baseband signal samples were generated, consistent with the description of the e-Czas signal structure presented in Section 2, with a sampling resolution of 1 µs. The stability of the internal reference oscillator in the SMU200 is much below required, therefore, this generator was clocked using 10 MHz and 1 PPS signals from the FS725 rubidium clock from Stanford Research Systems. The declared accuracy of FS725 is $\pm 5 \times 10^{-11}$ and the annual ageing is 5×10^{-10} [32]. In the set-up presented in Fig. 6, FS725 was driven by 1 PPS pulses from the GNSS receiver of the same type as is used in e-Czas signal receivers, which allows for synchronisation of the 1 PPS output pulses from FS725 with the GPS time base and slow tuning of 10 MHz clock with a very long time constant of 18 hours. Therefore, FS725 acts as a precise clock source and filter that reduces short-term jitter in GNSS-derived 1 PPS pulses for SMU200. The 1 PPS signal from FS725 is used to trigger the repetition of the e-Czas packet in a baseband arbitrary waveform generator every 3 seconds, giving the correct signal time structure.

All tested receivers showed a systematic error in the measurement of the packet reception time of about +13 µs regardless of the power level, with small differences (up to 2 µs) between individual receiver units. This error is most probably caused by the signal delay in the low-pass filter before the amplifiers and in the ADC converter and can be compensated for by appropriate constant correction. For comparison, simulations of the 5$^{\text{th}}$ order LC low-pass filter implemented in the receivers show a group delay of more than 5 μs with a strong dependence on the inductance/capacitance values of the components, which justifies the observed variability of the average time measurement error between devices due to variability of the LC parameters.

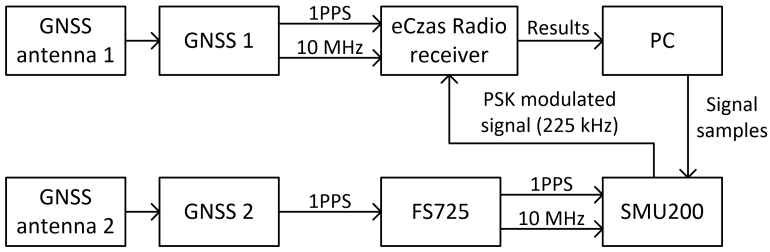

Fig. 6. Test set-up for receiver performance measurements.

The spread of the results, expressed as standard deviation σ_t of the measured packet time of arrival from 10-minutes long measurement series is presented in Fig. 7. It should be emphasised that the test signals were prepared taking into account the interpretation of the nominal time of the e-Czas packet emission presented in Section 3. Such a procedure involves the risk of making the same mistake twice: when implementing the receivers and when building a station for measuring their parameters. However, if the actual time of starting the packet emission from Solec Kujawski is different from the assumptions made, the receivers will return the results of the packet arrival time measurements with a systematic error, easy to assess and compensate after starting to record the real signals.

Taking into account the declared accuracy of end-user device synchronisation of 10 ms, the results presented in Fig. 7 prove that the possible quality of time dissemination using the e-Czas Radio service will not be limited by the sensitivity of the receivers. Sub-microsecond precision of phase-modulated radio packets, achieved for the signal level above –61 dB is encouraging, especially compared with the carrier period equal to 4.4 μs. It should also be noted that the signal time of arrival is not estimated from the carrier phase, as in phase-based positioning systems, but from variation in phase caused by modulation. Therefore, resolution and precision of both the method of signal emission from the LF transmitter in Solec Kujawski and the method of time measurement implemented in proposed receivers outperform the possible quality of time

dissemination, which in the case of LF signal propagation in real environment will be limited by variable propagation path characteristics and noise, both natural and man-made. The study of these factors is the main goal of building the described receiver network.

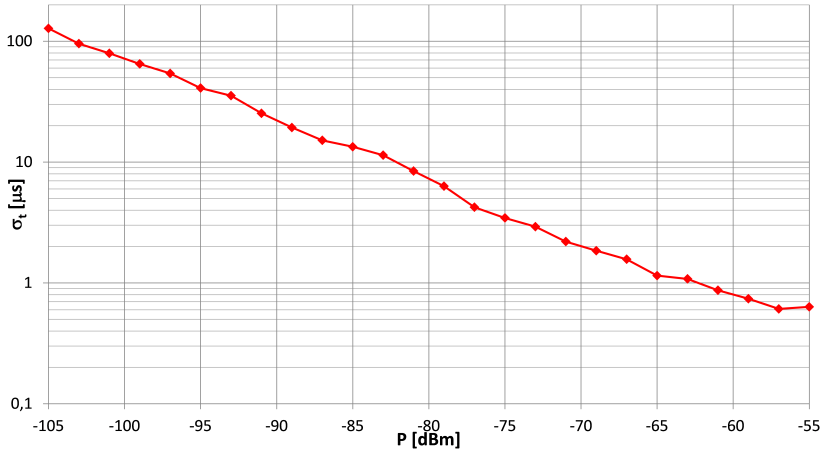

Fig. 7. Standard deviation of the e-Czas packet time measurements as a function of the signal power level for the test signal generated using the R&S SMU200.

The receiver sensitivity tests in the laboratory showed that even at the lowest level of the test signal of –105 dBm, at which time the measurement quality was much below expectations, all radio packets were demodulated without a single bit error, allowing for correct decoding of the content of all packets even without using Reed-Solomon decoding (correct CRC checksum without R-S error correction). Therefore, the quality of decoding the content of e-Czas messages, including timestamp and auxiliary data such as transmitter status, is not limited by the receiver sensitivity caused by internal noise either. Based on tests of the actual signal reception from Solec Kujawski, the author expects that the main source of possible message decoding errors will be industrial interferences and lighting discharges caused by storms near the receiver location. Thus, no reception error receiver characteristics are presented as BER/PER curves obtained for AWGN noise in a laboratory would not correspond to the expected conditions of real signal reception.

4.3. Real signal reception

Although the e-Czas Radio transmitter is operational and provides stable reception of time messages with millisecond-level accuracy, it happens that the observed parameters of emission are changed within small limits by the system operator. Therefore, an assessment of the absolute time of signal reception should not yet be performed. However, some insight into the possible accuracy of end-user device synchronisation can be obtained from the analysis of dispersion of the e-Czas signal time of arrival during reception under stable conditions. For this purpose, the measuring receiver was installed at the Gdansk University of Technology with a loop antenna on the roof of the faculty building, at a distance of approximately 150 km from the transmitter. During the test, the received signal power level was approx. –65 dBm with about 4 dB changes caused by the dynamic power control implemented in the transmitter in Solec Kujawski. Figure 8 contains a histogram of the received time of arrival of over 6600 packets received during a 10-hour measurement campaign, presented with respect to the average time. The standard deviation of the results was 18.47 μs, and 99.57 % of the results were within ±55 μs range.

The observed asymmetric distribution of results in Fig. 8 is caused by the combined effect of:

– radio wave propagation phenomena,
– residual modulation from AM DSB modulation sidelobes,
– interferences in the reception bandwidth,
– receiver noise.

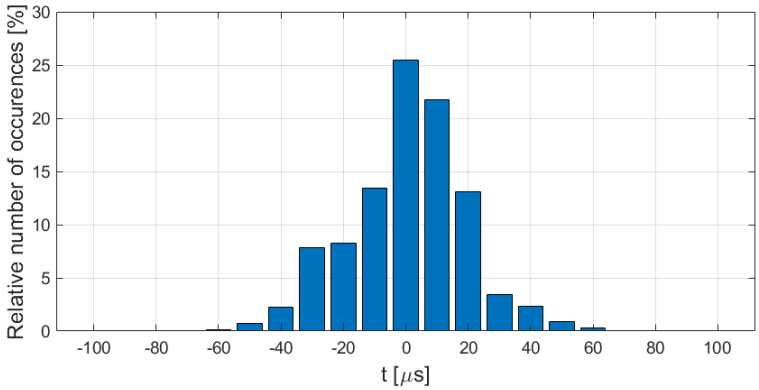

Fig. 8. Histogram of deviation of the e-Czas Radio signal time of arrival measurements with respect to the mean value.

It is not possible to separate these effects using a single receiving site; therefore, a network of several synchronised receivers is needed. For example, the estimation of the residual modulation effect will be performed by installing one receiver in close proximity to the transmitting site, while man-made interferences can be significantly reduced by signal reception using another receiver placed in a rural area. The possible time variability of AM modulation justifies the need for synchronous reception of the same e-Czas signal at different sites, as it allows for data subtraction for relative measurements, which removes correlated effects from the processed data. This feature was used to test the receiver noise effect using two receivers installed at the same location at the Gdansk University of Technology, which received signals not only with the correlated effect of AM modulation, but also with correlated interference and propagation effects. Fig. 9 shows the distribution of differences in the message time of arrival measurements performed by both receivers.

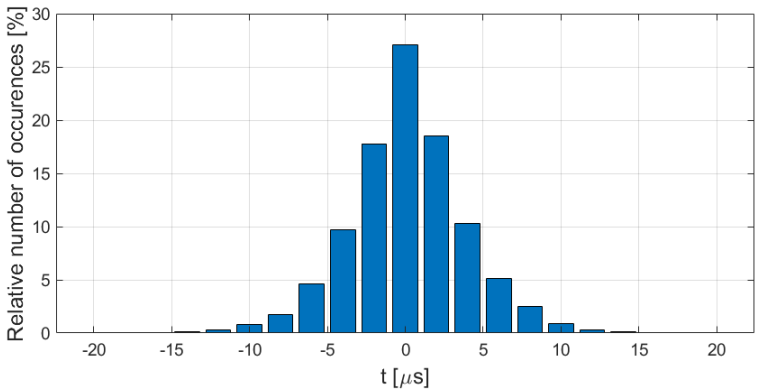

Fig. 9. Example histogram of the difference in packet detection time by two receivers installed in the same place.

The average difference between the results from the two receivers was below 0.2 μs with a standard deviation of only 3.79 μs. The histogram in Fig. 9 shows good agreement with the Gaussian distribution, which confirms that the receivers engineered do not introduce any systematic bias or excessive measurement errors that cannot be explained by the receiver internal noise. The presented results demonstrate the possibility of obtaining consistent results from the e-Czas receiver network under repeatable conditions with accuracy comparable to the quality of time synchronization that can be achieved using the NTP protocol in local computer networks [6, 37] or DCF77 radio signal [13].

5. Conclusions

Despite the launch of the e-Czas Radio service, to date no measurement data has been published that would allow the verification of the quality of time distribution and the achievable accuracy of synchronisation of devices using the time signal transmitted by the LF transmitter in Solec Kujawski. To fill this gap, a set of four receivers was built, forming a network of receivers that measures the time of arrival of the e-Czas messages together with a central server and database for data acquisition and processing. The network of receivers will be used for an independent evaluation of performance of the e-Czas system. The results of measurements performed using the proposed receivers may contribute to the wider use of this method of the official Polish time dissemination.

References

[1] Lu, Q., Feng, X., & Zhou, C. (2021). A detection and weakening method for GNSS Time-Synchronization attacks. *IEEE Sensors Journal*, *21*(17), 19069–19077. https://doi.org/10.1109/jsen.2021.3088138

[2] Radoš, K., Brkić, M., & Begušić, D. (2024). Recent advances on jamming and spoofing detection in GNSS. *Sensors*, *24*(13), 4210. https://doi.org/10.3390/s24134210

[3] Felux, M., Fol, P., Figuet, B., Waltert, M., & Olive, X. (2024). Impacts of Global Navigation Satellite System jamming on aviation. *NAVIGATION Journal of the Institute of Navigation*, *71*(3), navi.657. https://doi.org/10.33012/navi.657

[4] Mills, D., Martin J., Burbank, J., & Kasch, W. (2010). *Network Time Protocol Version 4: Protocol and Algorithms Specification*. RFC 5905. https://doi.org/10.17487/rfc5905

[5] IEEE Standard for a Precision Clock Synchronization Protocol for Networked Measurement and Control Systems, in *IEEE Std 1588-2019 (Revision of IEEE Std 1588-2008)*, pp.1-499, 16 June 2020, https://doi.org/10.1109/IEEESTD.2020.9120376

[6] Firose, F. F., Agarwal, A., Sharma, D., Yadav, D. S., & R, S. M. (2025). Time Synchronization Performance Analysis based on NTP Data Captured from Two Distant Locations. In *2025 International Conference on Innovation in Computing and Engineering (ICE)* (pp. 1–6). https://doi.org/10.1109/ice633092025.10984309

[7] Miškinis, R., Jokubauskis, D., Smirnov, D., Urba, E., Malyško, B., Dzindzeleta, B., & Svirskas, K. (2014). Timing over a 4G (LTE) mobile network. In *28th European Frequency and Time Forum*. https://doi.org/10.13140/RG.2.1.1339.2081

[8] Liang, K., Yang, Z., Fang, W., & Wang, J. (2023). Performance characterization of network timing with remote traceability via GNSS time transfer. *Measurement and Control*, *56*(7–8), 1387–1395. https://doi.org/10.1177/00202940231161568

[9] Rinaldi, S., Pasetti, M., Bonafini, F., Ferrari, P., Flammini, A., Sisinni, E., Artale, G., Cataliotti, A., Cosentino, V., Di Cara, D., Panzavecchia, N., & Tine, G. (2020). Design of a time dissemination system using CHIRP modulation for medium voltage smart grid applications. *IEEE Transactions on Instrumentation and Measurement*, *69*(9), 6686–6695. https://doi.org/10.1109/tim.2020.2975372

[10] Zaccaro, E., Ronchetti, L., Lometti, A., Troia, S., & Bregni, S. (2020). Performance evaluation of PTP synchronization networks for 5G Front/Mid-Haul Transport. In *2020 IEEE Latin-American Conference on Communications (LATINCOM)* (pp. 1–6). https://doi.org/10.1109/latincom50620.2020.9282341

[11] International Telecommunication Union (2024). *Radio Regulations. Articles*. https://www.itu.int/pub/R-Reg-RR

[12] Physikalisch-Technische Bundesanstalt. *DCF77 web page*. https://www.ptb.de/cms/en/ptb/fachabteilungen/abt4/fb-44/ag-442/dissemination-of-legal-time/dcf77.html

[13] Hetzel, P. (1988). Time dissemination via the LF transmitter DCF77 using a pseudo-random phase-shift keying of the carrier. *2nd European Frequency and Time Forum*. Neuchâtel. pp. 351–364.

[14] SYRTE – Observatoire de Paris, *ALS162 web page*, *Provision of the legal time by ALS162 signal*, https://syrte.obspm.fr/spip/services/ref-temps/article/mise-a-disposition-du-temps-legal-par-le-signal-als162?lang = en

[15] LNE-SYRTE Observatoire de Paris, *Attestation Exactitude du signal ALS162* (in French), https://syrte.obspm.fr/spip/IMG/pdf/2019_05_27_attestation_als162.pdf

[16] Portfolio of DCF77 receivers offered by Gude, https://gude-systems.com/en/radio-time-systems/dcf77-time-server

[17] Portfolio of DCF77 receivers offered by Meinberg, https://www.meinbergglobal.com/english/products/dcf77-long-wave-receiver.htm

[18] International Bureau of Weights and Measures, Time Department (2024). *Time Signals*, https://webtai.bipm.org/ftp/pub/tai/annual-reports/bipm-annual-report/TIMESIGNALS

[19] Portfolio of eLoran receivers offered by Reelektronika, http://www.reelektronika.nl/products/loradd-utc-series

[20] Portfolio of eLoran receivers offered by UrsaNav, https://ursanav.com/user-equipment

[21] Miś, T., Gruszczyński, M., & Czubla, A. (2024). 25th anniversary of RCN Solec Kujawski longwave radio station and the introduction of digital time signal in Poland. In *2024 4th URSI Atlantic Radio Science Meeting (AT-RASC)*. https://doi.org/10.46620/ursiatrasc24/ypxj8010

[22] Krzysztofik, W. (1994). The technical and social aspects of the LF Warsaw Broadcasting Station reconstruction. In *International Broadcasting Convention – IBC '94*. https://doi.org/10.1049/cp:19940808

[23] Webpage of "e-Czas Radio" project (in Polish). https://e-czas.gum.gov.pl/e-czas-radio

[24] Blue Dot Solutions website. https://www.bluedotsolutions.eu/index.php/en/time-synchronisation-module

[25] Polish Central Office of Measures. Dystrybucja czasu urzędowego na falach długich, przy wykorzystaniu fali nośnej 225 kHz Programu Pierwszego Polskiego Radia. Struktura ramki, przesyłane dane i ich przeznaczenie. Version 1.0. https://e-czas.gum.gov.pl/wp-content/uploads/2024/06/e-CzasPL-Opis-ramki-czasu-e-Czas-Radio.pdf (in Polish)

[26] Polish Central Office of Measures. Distribution of official time on long waves, using the 225 kHz carrier wave of the First Polish Radio Program. Frame structure, transmitted data, and its purpose. Version 1.0. https://github.com/e-CzasPL/TimeReceiver225kHz/blob/main/doc/PCSK-225%20-%20Distribution%20of%20official%20time%20on%20long%20waves.pdf

[27] Polish Central Office of Measures. Distribution of official time on long waves, using the 225 kHz carrier wave of the First Polish Radio Program. Description of the design of an exemplary receiver module for encrypted official time signals. Version 1.0, https://github.com/e-CzasPL/TimeReceiver225kHz/blob/main/doc/Simple%20Time%20Receiver%20for%20PCSK-225.pdf

[28] Ettus Research. *N200/N210 Knowledge Base*, https://kb.ettus.com/N200/N210

[29] Ettus Research. *LFRX Daughterboard 0–30 MHz*. https://www.ettus.com/all-products/lfrx

[30] Kiwi SDR web page. http://kiwisdr.com

[31] Stanford Research Systems. *FS725 Rubidium Frequency Standard. Operation and Service Manual*. Version 1.3 (2015). https://www.thinksrs.com/downloads/pdfs/manuals/FS725m.pdf

[32] Trimble Navigation Limited. Mini-T™GG Multi-GNSS Disciplined Clock. Data Sheet (2013). Archived in 2019: https://web.archive.org/web/20190923234615/http://trl.trimble.com/docushare/dsweb/Get/Document-781225/

[33] EURAMET Technical Guide No. 3 (2016). *Use of GPS Disciplined Oscillators for Frequency or Time Traceability*. Version 1.0. Available online: https://www.euramet.org/publications-media-centre/technical-guides

[34] Banerjee, P., Suman, N., Suri, A. K., Chatterjee, A., & Bose, A. (2007). A study on the potentiality of the GPS timing receiver for real time applications. *Measurement Science and Technology*, *18*(12), 3811–3815. https://doi.org/10.1088/0957-0233/18/12/016

[35] Mao, F., Lou, Y., Geng, C., Song, Q., Gong, X., & Gu, S. (2024). Evaluation of timing and time transfer with PPP using Galileo High Accuracy Service. *Measurement*, *226*, 114152. https://doi.org/10.1016/j.measurement.2024.114152

[36] Liu, M., Tu, R., Li, F., Chen, Q., Li, Q., Chen, J., Zhang, P., & Lu, X. (2024). GPS + 5G fusion for high-precision time transfer. *Measurement Science and Technology*, *35*(4), 045024. https://doi.org/10.1088/1361-6501/ad1d2f

[37] Novick, A. N., & Lombardi, M. A. (2015). Practical Limitations of NTP time transfer. In *2015 Joint Conference of the IEEE International Frequency Control Symposium & the European Frequency and Time Forum* (pp. 570–574). https://doi.org/10.1109/fcs.2015.7138909

Jaroslaw Sadowski received the M.Sc. degree in mobile radio communication systems from the Gdansk University of Technology, Gdansk, Poland, in 2002, the Ph.D. degree in radio communication in 2010, and the D.Sc. degree in informatics and telecommunications in 2019. His main field of study is localisation in indoor environments, ultra-wideband technology, and electromagnetic compatibility. From 2002 to 2006, he worked in industry designing and constructing 2G/3G base stations. Since 2007, he has been an Assistant Professor in the Department of Radio Communication Systems and Networks (DRCSN), Gdansk University of Technology. Since 2018, he has been the Deputy Head, and since 2020 the Head of the Department of Radio Communication Systems and Networks, Gdansk University of Technology. He is a member of the EMC Section of the Committee on Electronics and Telecommunications of the Polish Academy of Sciences.